

See discussions, stats, and author profiles for this publication at: <https://www.researchgate.net/publication/263980271>

Formation of Mixed Monolayers from 11-Mercaptoundecanoic Acid and Octanethiol on Au(111) Single Crystal Electrode under Electrochemical Control

ARTICLE in THE JOURNAL OF PHYSICAL CHEMISTRY C · NOVEMBER 2013

Impact Factor: 4.77 · DOI: 10.1021/jp406229f

CITATIONS

4

READS

78

6 AUTHORS, INCLUDING:



Zoilo González

Institute of Ceramics and Glass

29 PUBLICATIONS 53 CITATIONS

SEE PROFILE



Guadalupe Sánchez Obrero

University of Cordoba (Spain)

5 PUBLICATIONS 29 CITATIONS

SEE PROFILE



Rafael Madueño

University of Cordoba (Spain)

24 PUBLICATIONS 541 CITATIONS

SEE PROFILE



Manuel Blázquez

University of Cordoba (Spain)

76 PUBLICATIONS 884 CITATIONS

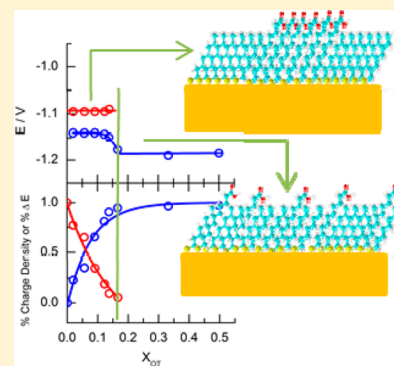
SEE PROFILE

Formation of Mixed Monolayers from 11-Mercaptoundecanoic Acid and Octanethiol on Au(111) Single Crystal Electrode under Electrochemical Control

Zoilo González-Granados, Guadalupe Sánchez-Obrero, Rafael Madueño, José M. Sevilla, Manuel Blázquez, and Teresa Pineda*

Institute of Fine Chemistry and Nanochemistry, Department of Physical Chemistry and Applied Thermodynamics, University of Cordoba, Campus Rabanales, Ed. Marie Curie 2ª Planta, E-14014 Córdoba, Spain

ABSTRACT: The formation process and characterization of mixed layers of 11-mercaptoundecanoic acid (MUA) and octanethiol (OT) on Au(111) single crystal electrodes under electrochemical control from alkaline solutions are analyzed in this work by means of electrochemical techniques such as chronocoulometry, cyclic voltammetry, and electrochemical impedance spectroscopy. The surface composition of the layers differs from the component ratio of bulk solution and is supposed to be directed by both the adsorption potential of the individual molecules and its adsorption behavior. The relative competitive adsorption capacity of the two functional groups in the bifunctional molecules plays an important role in the electrochemical deposition of mixed layers as the second component can occupy the free space that the first molecule liberates during reorganization. Two different mixed layers can be obtained under the experimental conditions of this work: a macroscopically homogeneous layer and a homogeneously mixed layer at higher and lower MUA:OT ratios. The macroscopically mixed layer should be formed by small domains that keep the same energetic as the single-component SAM of the thiol constituents, and the homogeneously mixed should be formed by few MUA molecules diluted in an OT layer.



INTRODUCTION

The preparation of self-assembled monolayers (SAMs) of sulfur-based molecules on gold substrates has been a topic to which great attention has been paid in the past decades.^{1–6} Interesting properties such as high stability, compactness, and flexibility in designing the distribution of terminal groups that endowed the SAMs with different functionalities have been proclaimed as good characteristics that made them promising systems for applications in biology, medicine, catalysis, and material chemistry.

Most of the functionalized SAMs are built from ω -alkanethiol derivatives, and the main problems encountered are the difficulty in obtaining well-organized layers due to the different size of the headgroup of the molecule in comparison with the alkane tail and, more importantly, the destabilization due to interactions of these groups that are sometimes able to break the van der Waals interactions between the parallel chains.^{7–9} It has recently been reported that the introduction of functional groups simultaneously alters the internal dipole moment and the geometry of the constituents being the final orientation of the dipoles in the monolayer the key aspect in determining the SAM properties.¹⁰

An interesting strategy to avoid these interactions is to dilute the layer with an n -alkanethiol derivative partner in a way that the functional groups can be homogeneously mixed. However, the final structure of the mixed SAMs is highly dependent on multiple factors such as chain length difference, nature of the functional group, and solvent used in the modification solution.

The phase behavior of two-component SAMs was first investigated from both theoretical and thermodynamic perspectives¹¹ concluding that at equilibrium with a solution containing a mixture of two components a SAM will not consist of regions of separated phases. The final single phase may contain only one alkanethiolate or a homogeneous mixture of the two components, being the strength of the lateral molecule interactions the primary factor in determining the composition of that phase. However, the experimental conditions necessary to achieve equilibrium are not easy to define. The characterization of mixed SAMs has since been directed to elucidate such phase behavior. Macroscopic measurements have suggested that the binary monolayers formed from molecules of similar chain length do not phase segregate into macroscopic islands, but they form molecularly mixed SAMs.^{12,13} Moreover, by using scanning probe microscopy, incomplete mixing has been observed. This state of miscibility has been called “macroscopically homogeneous” as it differs from the truly homogeneous state at the molecular level and from the state in which the segregation of the molecules gives place to different types of sizable domains.¹³ In this context, electrochemical techniques give us valuable information that, although macroscopic in nature, allow us to correlate with the microscopic view.¹⁴ The term “macroscopically phase-separated” has been defined to

Received: June 24, 2013

Revised: October 23, 2013

Published: October 24, 2013



describe the extent of the segregation which is enough to give two macroscopically different responses in techniques such as voltammetry of the reductive desorption within others.¹³

Kakiuchi's group has analyzed different binary SAMs composed of *n*-alkanethiols and ω -alkanethiols of different chain lengths and has established a correspondence between the macroscopic behavior as studied mainly by electrochemical techniques and the microscopic morphology. They found that the shape of the voltammetric curves for the reductive desorption process is very sensitive to the existence of nanometer scale domains in the SAMs, concluding that a number of 50 molecules occupying a single domain of around 15 nm² is required for exhibiting two-dimensional bulk properties.^{13–15} The behavior observed when using two pairs of different molecules is dependent on the difference in the number of methylene units. From voltammetric curves of the various combinations it has been found that the SAMs are macroscopically phase separated when the peak potential differences for the single-component SAMs are greater than 0.20 V.¹³ Thus, the "macroscopically homogeneous state" has been defined as a state that is somewhere between the truly homogeneous state at the single molecular level and a macroscopically phase-segregated one that is enough to give two macroscopically different responses in techniques such as voltammetry of the reductive desorption.

Apart from the problem of reaching the thermodynamic equilibrium that would be the way that the structure of a mixed SAM is reproducible, the time necessary to get this state is usually long for feasible applications. This fact has made some researchers to work under experimental conditions that allow obtaining a layer presenting good properties in a shorter time. In this sense, potential assisted deposition has been considered as a suitable method that speeds up the relatively slow passive adsorption. The method takes into consideration the anodic reaction that takes place to form the Au–S bond by contacting the thiol derivatives in solution with the clean gold surface.^{16–26}

In a recent work, we have reported the formation of monolayers of 1,8-octanedithiol on the Au(111) single crystal electrode by oxidative deposition from alkaline solutions under electrochemical control. The method resulted in the formation of very reproducible layers that contain mainly standing-up molecules, built in a shorter time than those formed by the spontaneous assembly from ethanolic solution.²⁷ In the present work, we extend the use of this methodology to tune the formation of mixed SAMs of 11-mercaptoundecanoic acid (MUA) and octanethiol (OT). We take advantage of both the different adsorption potential and the mechanism of these molecules to create layers with specific properties in a shorter time. The characterization of these mixed layers is carried out by using electrochemical techniques such as cyclic voltammetry, chronocoulometry, and electrochemical impedance spectroscopy.

EXPERIMENTAL METHODS

Chemicals. 11-Mercaptoundecanoic acid, octanethiol, potassium ferricyanide, and semiconductor grade purity potassium hydroxide were purchased from Sigma-Aldrich. The rest of the reagents were from Merck analytical grade. All solutions were prepared with deionized water produced by Millipore system.

Methods. A conventional three-electrode cell comprising a platinum coil as the counter electrode, a 50 mM KCl calomel electrode as the reference electrode, and a gold single crystal

(111 face) as the working electrode was used. The Au(111) single crystal electrode was a homemade hemisphere of approximately 2 mm diameter with a gold wire, mounted at its far tip, that allows easier handling of the crystal. Before each electrochemical measurement, the electrode was annealed in a natural gas flame to light red melt for about 20 s and, after a short period of cooling in air, quenched in ultrapure water. The electrode was then transferred into the electrochemical cell with a droplet of water adhering to it to prevent contamination. The surface condition was confirmed by a cyclic voltammogram in 0.01 M HClO₄, and the real surface area was determined from the reduction peak of oxygen adsorption on the Au electrode. This surface treatment was the most appropriate to produce a surface that is clean, ordered, and highly reproducible.

Cyclic voltammetry (CV), chronocoulometry, and capacitance–potential (*C*–*E*) curves were recorded on an Autolab (Ecochemie model Pgstat20) instrument attached to a PC with proper software (GPES and FRA) for the total control of the experiments and data acquisition.

RESULTS AND DISCUSSION

"In Situ" MUA–OT Mixed Layer Formation under Electrochemical Control. Figure 1 shows a comparative view

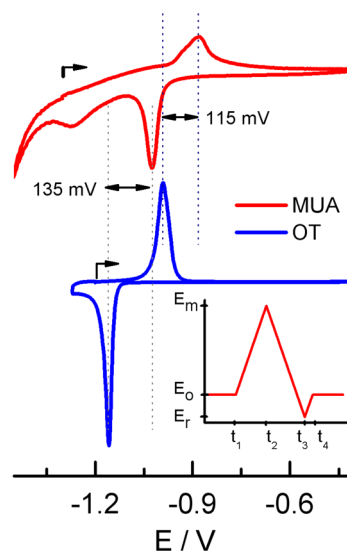


Figure 1. Cyclic voltammetry of a Au(111) single-crystal electrode in a 1 mM MUA (top) and OT (bottom) in 0.1 M KOH solutions; $V = 20$ mV/s. Inset: scan program. The arrows in the voltammetric curves indicate the position of E_0 and the scan direction.

of the cyclic voltammograms recorded in solutions of either 1 mM MUA or 1 mM OT in KOH 0.1 M with a Au(111) single crystal electrode. The electrochemical signals were obtained (see scheme in the inset of Figure 1) starting at a potential (E_0) chosen as one at which the thiol derivatives are not expected to bind to the gold surface. After stabilization of the electrode current intensity, the potential was scanned in the positive direction (at 20 mV/s) up to reach a potential (E_m) where it was reversed. The general features of these voltammetric curves are similar, both exhibiting an oxidation and a reduction peak that correspond to the adsorption of the molecules through the formation of an S–Au bond and its subsequent desorption, respectively. However, the adsorption behavior of these molecules under these experimental conditions looks very different. First, the lower adsorption potential for OT

molecules with respect to MUA (-0.99 V for OT and -0.875 V for MUA) is indicative of an improved stability of the assembled OT film. As the anodic formation reaction is taking place in alkaline medium, the terminal negative carboxylic acid group of MUA adds to the thiolate ones and contributes to the destabilization of the layer. Second, the charge density involved in the case of MUA ($\approx 45 \mu\text{C}/\text{cm}^2$) does not correspond to the formation of a complete layer of standing-up molecules on the surface,²⁸ while for OT ($\approx 72 \mu\text{C}/\text{cm}^2$) full coverage is reached. It is interesting to note that even if the scan rate is lowered to 2 mV/s , the charge density corresponding to full coverage is not obtained for MUA. The reason for this can be found in the presence of a second functional group in the MUA molecule that should compete for the interaction with the surface as it was reported for octanedithiol.²⁷ Another analogy with the case of bifunctional molecules is the occurrence of a certain anodic current at potentials positive to the adsorption peak that is ascribed to the reorganization of the molecules on the surface from a lying-down to a standing-up orientation giving place to some adsorption events and, in this way, a higher charge density in the subsequent reductive peak ($\approx 65 \mu\text{C}/\text{cm}^2$) in comparison to the oxidative one. This, again, is in contrast to the CV of OT that shows no current at all at the potentials positive to the adsorption peak and a similar charge density for adsorption and desorption processes.²⁷

An important difference in the shape of the voltammograms is observed in the potential region negative to the peaks. The tilted shape of the CV for MUA and the presence of a small reduction peak negative to the main reductive desorption process evidence a more complex behavior of MUA with respect to OT and ODT.²⁷ In fact, this peak appears under all the experimental conditions either “in situ” or “ex situ” for desorption of MUA layers. The origin of this peak is unknown at the moment, but it should have some influence in the adsorption behavior of this molecule (note that some negative current is also obtained at the potential E_0). We assume, however, that it has not relation with the formation or breaking of the S–Au bond. On the other hand, the potential of zero charge of the MUA and OT SAMs are -0.42 and -0.51 V, respectively;²⁹ therefore, similar negative charge density is expected in this potential region for the two layers. In the case of carboxylic acids, they adsorb on gold only when highly positive potentials are applied,^{30–33} but the competitive adsorption under the present conditions cannot be neglected.

Taking advantage of the observed differences in their adsorption behavior for these two molecules on Au(111) surfaces, we have intended the formation of mixed monolayers by using the same protocol. On the basis of the main differences in adsorption, as commented below, we design experiments with the objective to obtain mixed layers of the appropriate composition ratio. In a first approximation, it can be taken in mind that the OT molecules that adsorb to the gold surface at lower potentials than MUA ($\Delta E_p = 115 \text{ mV}$) are able to complete the layer before the latter might bind, as deduced by the potential at which the current for OT reaches the zero value at the high potential side of the anodic peak (Figure 1). Then, we have recorded the electrochemical signal for different mixtures of MUA/OT as indicated in Figure 2. As can be observed, the presence of low amounts of OT does not substantially change the shape of the peak. As the adsorption of thiolate groups, either spontaneously or under potential control, depends on the thiol concentration, it can be said that few OT molecules are able to bind to the surface in the

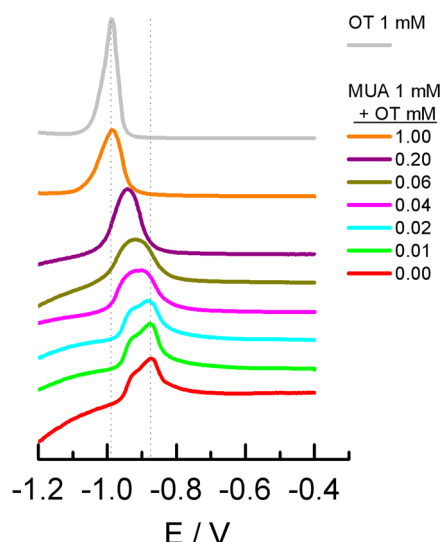


Figure 2. Voltammetric curves for the formation of mixed layers in the presence of different MUA:OT concentration in 0.1 M KOH solution; $V = 20 \text{ mV/s}$.

time window of the experiment, and the layer is almost formed by MUA under these experimental conditions. However, at higher OT concentration (0.04 mM), the peak changes in both shape and potential, indicating a competition between the molecules for the gold sites. The progression of the peak potential to that of the pure OT is accompanied by the total suppression of the current at positive potential values as well as the peak at potentials negative to the main reductive peak. Moreover, in general, the tilting of the voltammogram is significantly reduced. The charge density of the peaks corresponding to the mixed layers increases up to values very close to that of OT. (The reductive desorption voltammogram of the layer obtained in the presence of 1 mM OT and 1 mM MUA is $66 \mu\text{A}/\text{cm}^2$, very close to that of pure OT that is $74 \mu\text{A}/\text{cm}^2$. However, the higher half-width of the former (72 mV vs 46 mV for OT) is an indication of the existence of some disorder on the layer as a consequence of its mixed nature.)

A different way to build up the molecular layer by using a potentiostatic method has been tried.²³ The method follows the potential program depicted in the inset of Figure 3. It consists of stepping the potential from a value negative to the anodic peak ($E_0 = -1.35 \text{ V}$; $t = 120 \text{ s}$) where no adsorption of molecules occurs to a value comprised in the positive branch of the voltammogram ($E_{\text{for}} = -0.4 \text{ V}$; $t = 600 \text{ s}$) where it is maintained for a time that is considered enough for a stable layer formation. After this time the potential is scanned, and a voltammetric curve is recorded. In Figure 3, the cathodic branches of the voltammograms are shown as a function of the ratio MUA/OT in the solution. As can be observed, the reductive peak signal obtained under these conditions evidences that the layer composition is more sensitive to the presence of a certain amount of OT molecules in the solution than that deduced from the shape of the adsorption peaks (Figure 2). Moreover, the change in desorption potential takes place from the lower ratio probed.

The characteristic parameters such as peak potential and half-width for the adsorption and desorption processes are plotted in Figure 4. The peak potentials decrease with the increase of OT concentration in solution from the lowest concentration tested and reach the value for the pure OT layer when both

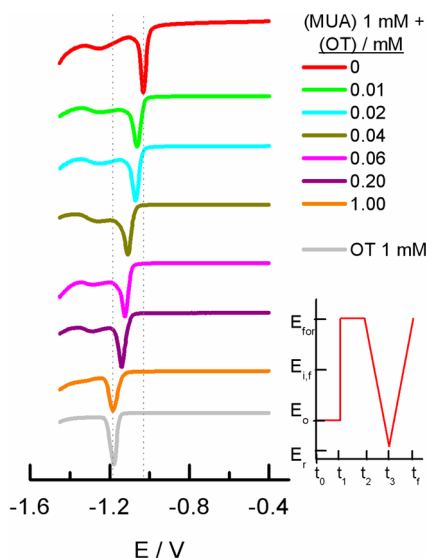


Figure 3. Voltammetric curves for the reductive desorption of mixed layers formed by using the potential programs shown in the inset, in the presence of different MUA:OT concentration in 0.1 M KOH solution; $V = 20$ mV/s.

molecules are in a 1:1 ratio. The inset in Figure 4 compares the normalized change in potential ($\% \Delta E$) for the layer formation and destruction processes. The data trend indicates that the peak for the formation of the layer from a mixture of MUA and OT in solution is less sensitive to the presence of OT than the peak for the destruction process. As commented above, the anodic peak shows the adsorption of the molecules in solution during the time that the electrode potential is swept in the region of OT adsorption, whereas in the potentiostatic methods

a negative potential is used that allows the competitive adsorption of both thiol derivatives.

An interesting behavior is observed in the half-width trend. The values for the adsorption peak increase sharply at low OT concentration, reaching a maximum when the MUA:OT ratio is 20:1. At lower ratios, the half-width decrease but do not reach the value for the pure OT layer. The reduction peak potentials follow the same trend observed for the oxidation peaks. However, the half-width shows a small variation in comparison to the anodic peak, keeping an average value of 37 mV.

“Ex Situ” Characterization of the Mixed MUA–OT Layers Formed under Electrochemical Control. The characterization of the mixed layers formed under electrochemical control is carried out by “ex situ” experiments. In this case, we have carried out chronocoulometric curves in order to check the process of layer formation. Thus, immediately after the potential program is finished, the modified electrodes were removed from the formation solution and transferred to the electrochemical cell containing only supporting electrolyte. Under these conditions, the cyclic voltammograms for the reductive desorption process shown in Figure 5 are obtained. A similar trend to that found when the voltammograms were recorded in the presence of the thiol mixture is also observed. However, when the OT concentration increases, reaching a MUA/OT solution ratio lower than 6/1, an unexpected result is obtained. It is found that the potential for the reductive desorption is lower than that for the pure OT layer. Upon decreasing the molar ratio, the potential goes more negative (Figure 6) reaching the value of the longer dodecanethiol (DDT) SAM. This potential change to negative values is interpreted as due to a more organized layer formed under these lower solution ratios.

It is worth to mention that under all the experimental conditions explored in this work no peaks originated from

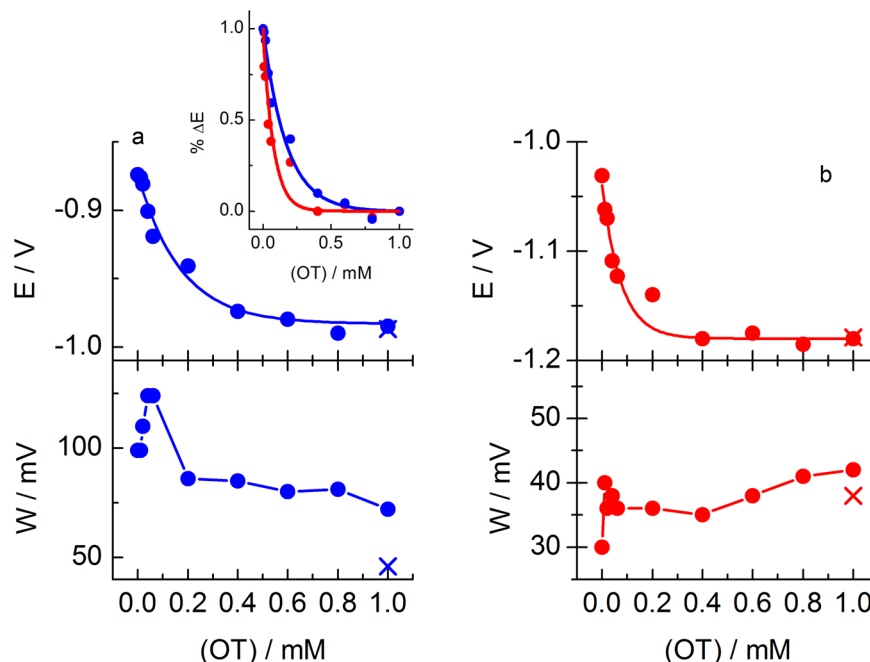


Figure 4. Changes in the peak potential (E) and half-width (W) for the formation (a) and the reductive desorption (b) peaks of the mixed MUA–OT layer formed under potentiodynamic conditions and at fixed potential, respectively, as a function of the OT concentration in solution. [MUA] = 1 mM. The cross symbols are used to indicate the parameters for a pure OT–SAM layer. Inset: normalized changes in the peak potentials for the formation (blue) and reductive desorption (red) from the data in (a) and (b), respectively.

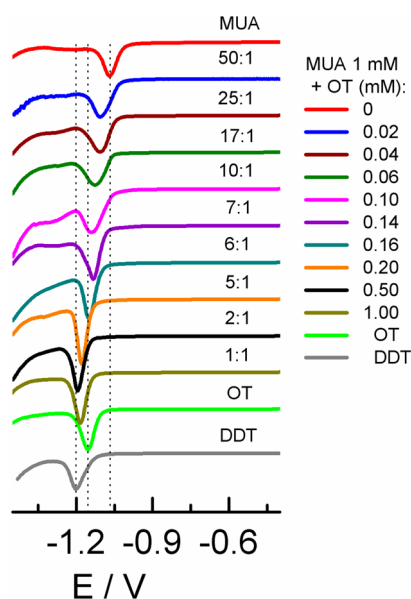


Figure 5. Voltammetric curves for the reductive desorption of the mixed layer formed by using the potential programs shown in the inset of Figure 3 at different MUA:OT ratios. After modification the electrode is transferred to an electrochemical cell containing 0.1 M KOH. The voltammograms were recorded after 15 min equilibration with the working solution at the initial potential of -0.4 V; $V = 20$ mV/s.

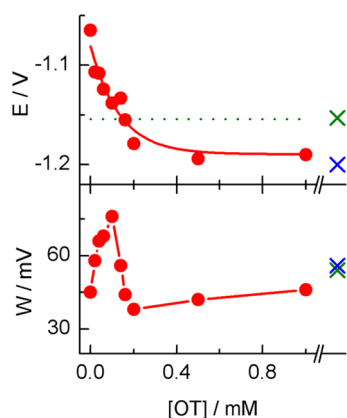


Figure 6. Changes in the peak potential (E) and half-width (W) for the reductive desorption peaks of the mixed MUA–OT layers of Figure 5. The green crosses correspond to the parameters for desorption of a pure OT monolayer and the blue ones to those of DDT. The dotted green line is drawn to note the increased stability of the mixed MUA–OT layers with respect to OT.

phase-separated domains are observed as it is expected based on reported observations.¹³ In contrast, a broadening of the reductive desorption peak at higher molar ratios taking place simultaneously with the potential displacement can be detected. An explanation for this behavior can be that in the presence of low OT concentrations the layer contains a small amount of OT molecules that although can form phase-separated domains, the potential difference of the domains is so small that the merged peaks corresponding to desorption of each phase cannot be resolved. In fact, the narrowing of the desorption peaks is interpreted as strong and attractive interactions between molecules³⁴ and, therefore, the observation of broader peaks should be indicative of the weakening of

the lateral interactions probably due to a higher disorganization. It is interesting to note that this features have also been observed in the “in situ” experiments (see Figure 4), thus pointing to the existence of a specific mixed behavior under these MUA/OT molar ratios.

At higher OT concentration, the amount of MUA molecules in the mixed film is very low, and the nanosize domains could transform into a homogeneous mixed layer of MUA/OT. In fact, the sharpening of the peak (see Figures 5 and 6) in the cyclic voltammograms at ratios lower than 6/1 can be an indication of desorption of such a homogeneous layer. It could be also speculated that under this surface diluted state the MUA molecules that should be deprotonated in this medium (KOH 0.1 M) would not suffer the repulsive interactions that take place in a domain of pure MUA molecules, thus forming a more stable and better organized layer than that built up at higher MUA/OT ratios. For comparison, the cyclic voltammogram for desorption of the layer formed from pure DDT, under the same experimental conditions, is also shown in Figure 5. The desorption potential is almost coincident with those found for the mixed layer at low ratios. As the peak reduction potential reflects the difference in Gibbs energy of desorbed thiulates,³⁵ this behavior indicates a similar stability for the mixed SAMs under these conditions and the homogeneous DDT-SAM. A negative shift of the reductive desorption peak has been explained as an ideal mixing of the constituents in molecular dimensions.³⁶

Comparing Figures 4b and 6, we note, however, that the increased stability observed when the reductive desorption experiment is carried out under “ex situ” conditions can be explained by the additional time that the SAM stays in contact with the 0.1 M KOH solution. In fact, after the modified electrode is removed from the solution containing the thiol (either single or mixed components), it is rapidly rinsed with water and introduced in the electrochemical cell containing 0.1 M KOH. Before recording the CV, the system is allowed to equilibrate for at least 15 min at controlled potential (-0.4 V). In this period of time, the monolayer gains stability probably by repairing some conformational defects. As the solution does not contain free thiol molecules, refill of the defects is completely discarded. We can conclude that this equilibration step acts as an annealing of the mixed layer.

From the results described above, it can be concluded that the formation of a mixed monolayer from a solution of different concentration ratios of MUA and OT under electrochemical control results in mixed SAMs that are enriched in OT. This behavior is expected on the basis of their different oxidation potential that favors the chemisorption of OT by 115 mV (on average) (Figure 1). Moreover, the adsorption behavior of MUA described above should delay the appropriate chemisorption of these molecules and allow the additional entrance of new OT in the free space that the MUA can create during its reorientation process.

In an attempt to quantify the amount of each component in the mixed layer, we have deconvoluted the voltammetric curves included in Figure 5 by using two Gaussian functions. As is shown in Figure 6, the desorption peaks broaden up to reach a maximum value in the presence of 0.1 mM OT and then decrease to the values close to the peak for OT. The starting point is that the individual voltammetric peaks should conserve the peak potential and the average half-width for the pure components through the mixed SAM. In Figure 7, the potential and charge density for the individual peaks obtained in the

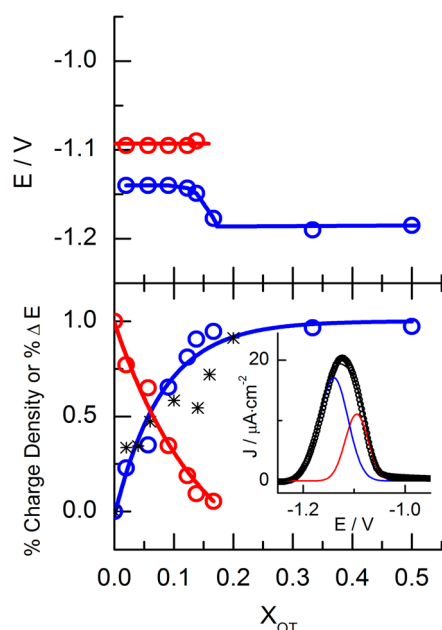


Figure 7. Changes in the peak potential (E) (top) and charge density percentages (bottom) for the individual peaks obtained in the deconvolution of the experimental desorption peaks of the mixed MUA–OT layer of Figure 5. The percentage of change in the experimental peak potential is also plotted (*). The inset shows the fitting results for the curve corresponding to $X_{OT} = 0.1$ including the individual components (red: MUA; blue: OT) and the theoretical total fitting curve.

deconvolution analysis are plotted. It is interesting to note that the analysis can be made using two peaks only at molar fractions of OT lower than 0.16. At higher values, the voltammogram gets sharper and can be fitted with only one peak. Under these circumstances the peak potential needs to be changed by ~ 40 mV. The trends followed by the charge densities for the individual peaks indicate that the ratio of MUA in the layer decreases very fast in a parallel fashion with the increase of OT, and at molar ratios higher than 0.16, the signal corresponds almost completely to OT. The presence of some MUA molecules in the layer is assumed although it should be very small to be detected by the voltammetric technique. This finding, together with the above-mentioned potential displacement (Figure 5), should be taken as an indication of the formation of an ideal mixed monolayer,³⁶ in place of a single OT–SAM under these experimental conditions. In Figure 7, the percentage of change in the peak potential ($\% \Delta E$) as a function of OT molar fraction for the experimental reductive desorption peak (Figures 5 and 6) is compared to the values of charge density corresponding to OT desorption. The same trend is obtained confirming the hypothesis of the evolution to the enrichment of the layer in OT when the layer is formed in the presence of very low OT concentration. From these data, we can hypothesize that under these experimental conditions a macroscopically homogeneous film composed of individual phases in the nanoscale contributing each with one peak to the broad signal followed by a redissolution of the MUA phase to form a layer homogeneously mixed at the molecular level are formed in the presence of low and high OT concentration, respectively.

This analysis allows us to distinguish two different types of mixed layers. On one hand, at higher MUA ratio, the mixed monolayer can be considered as “macroscopically homoge-

neous” in the sense that keeps the Gibbs energy of the individual components. However, in the region of lower MUA ratio, a homogeneously mixed MUA–OT layer is obtained which should contain a very low number of MUA molecules to be detected in the reductive desorption peak, but their presence in the SAM is evidenced by the higher Gibbs energy of the layer.

Taking in mind these ideas, we have further characterized the mixed MUA:OT layers representative of these two cases by using electrochemical impedance spectroscopy: these are the ratios (10:1) and (1:1) and are compared to the individual MUA and OT–SAM.

Electrochemical Impedance Spectroscopy. The electrode double-layer capacitance curves (C – E) are used to characterize the SAM compactness and thickness. The capacitance curves shown in Figure 8 were obtained by

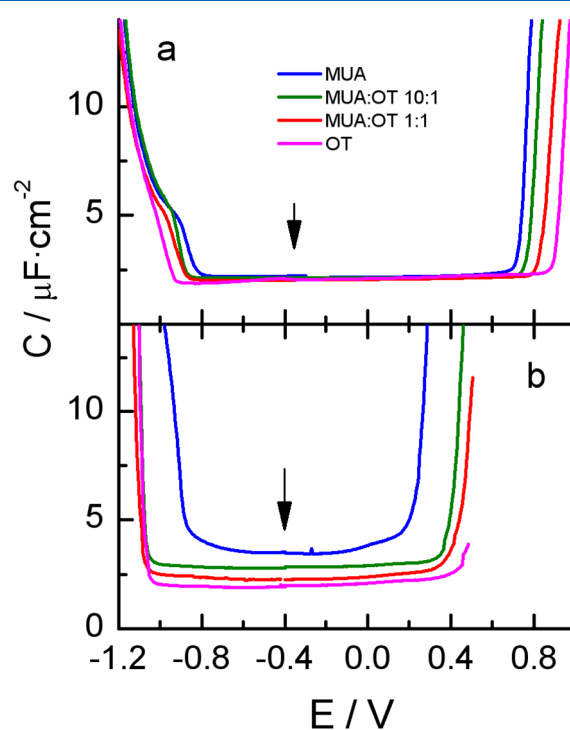


Figure 8. Differential capacitance–potential curves for the MUA, OT, and MUA:OT layers formed by electrochemical control in free thiol solutions: (a) 0.1 M sodium phosphate at pH = 7 and (b) 0.1 M KOH. Every curve is composed of two branches recorded in the direction of high and low potentials, respectively, with a freshly prepared monolayer. The arrows indicate the starting potential.

previously forming the layers under electrochemical control by holding the potential at -0.4 V for 600 s in the presence of the different MUA–OT ratios, as indicated in the figure legends. Each curve was recorded by starting at -0.4 V and the potential scanned to negative or positive values up to the region where the reductive or oxidative desorption takes place, respectively, either in 0.1 M KOH or in potassium phosphate 0.1 M at pH 7.0 (Figure 8). In the C – E curves recorded in alkaline media, the capacitance value in the stability potential range of the SAMs is maintained low and constant in respect to the potentials for layer destruction, and it is dependent on the mixed SAM composition (Figure 8b). As expected, the higher value ($C = 3.5 \mu\text{F}/\text{cm}^2$) corresponds to the pure MUA layer that should exhibit a charged surface under these experimental

conditions. The introduction of some OT molecules in the MUA layer, as can be assumed for the layer formed at a MUA/OT ratio of 10:1, brings about an important decrease in capacitance ($C = 2.95 \mu\text{F}/\text{cm}^2$) and an increase in the potential interval for the monolayer stability. The capacitance value also decreases when the layer was formed in a solution that contained a higher concentration of OT ($C = 2.22 \mu\text{F}/\text{cm}^2$). The curve obtained for a MUA/OT ratio of 1:1 is almost similar to that obtained for pure OT ($C = 2.05 \mu\text{F}/\text{cm}^2$).

On the other hand, we have measured the capacitance curves for the layers formed under the same conditions of Figure 8b but equilibrated and recorded in a neutral medium (potassium phosphate 50 mM, pH 7.0). As can be observed, the capacitance value obtained for all the layers in the wider potential range of stability is the same for all the layers ($C = 2 \mu\text{F}/\text{cm}^2$).

The low and constant capacitance values indicate the presence of a compact layer in the potential range where they are studied. This layer behaves as an ideal dielectric that can be analyzed by using the model of the double-layer capacitor ($1/C = d/\epsilon_r\epsilon_0$, where C is the double-layer capacitance, d the layer thickness, ϵ_0 the permittivity of the free space, and ϵ_r the relative permittivity of the layer). Assuming that the monolayers are formed by the alkanethiol molecules (either MUA or OT) in an all-trans configuration for the hydrocarbon chains with a tilt angle of 30° ,³⁷ the thickness can be determined by using the equation $d = 1.3 \times 10^{-8} n \cos \theta$, where n is the number of methylene units in the chain and θ the tilt angle. Then, by using the model of the double-layer capacitor, the ϵ_r values can be determined. The values obtained from the different capacitance values are gathered in Table 1.

Table 1. Monolayer Relative Permittivity for the Different Layers Prepared under Electrochemical Control

layer	capacitance ($\mu\text{F cm}^{-2}$)	ϵ_r
MUA	3.50	6.6
MUA:OT (10:1)	2.95	5.4
MUA:OT (1:1)	2.22	4.1
OT	2.05	3.0

Considering that in these systems the total differential capacity of the interface is divided into contributions from the film, the ionizable headgroups, and the diffuse part of the double layer,³⁸ the relative permittivity determined should be taken as an average of the film quality. In this way, it is interesting to note that the decrease of ϵ_r up to values close to the OT-SAM in alkaline media is an indication of the compactness and organization of the monolayer under these conditions.

On the other hand, the capacitance values for the layers at pH 7 are somewhat lower than those in alkaline media as it is expected taking into account the different protonation state of the layers containing carboxy terminal groups. We have carried out pH-titration curves of capacitance at a potential where the monolayers are stable in order to check if these measurements were sensitive to the monolayer protonation state. However, we do not find a good correlation since the capacitance values are very similar in both alkaline and neutral media. Then, we have used another strategy that has shown to be more sensitive to the layer protonation properties, as it is the electrochemical titration curve of the response of the negatively charge

ferricyanide ion by using electrochemical impedance spectroscopy.^{39,40}

SAMs of alkanethiols and ω -functionalized alkanethiols can block electron transfer between the electrode and electroactive redox species dissolved in an electrolyte solution.^{41–44} These studies have revealed that the heterogeneous electron transfer rate constant decays exponentially with the alkyl chain length, providing an efficient barrier toward heterogeneous electron transfer and ion penetration. Electron tunneling can take place in the monolayer, but in most cases, the electron transfer across the full width of the blocking monolayer is masked by faradaic reactions of molecules penetrating the monolayer either at pinhole or at defect sites.⁴⁵ On the other hand, the terminal groups in the monolayer may affect electron transfer. In this case, the electrostatic interactions between the solution redox species and the charged terminal groups in the monolayer govern their own redox response.^{46–49}

The impedance data for ferricyanide obtained in this work were analyzed using the Randles equivalent circuit, and the charge transfer resistance (R_{CT}) was determined as a function of solution pH.⁵⁰ Figure 9 shows the typical R_{CT} titration curve of 1 mM $\text{Fe}(\text{CN})_6^{3-/4-}$ at the MUA, mixed MUA:OT, and OT layers at different solution pHs.

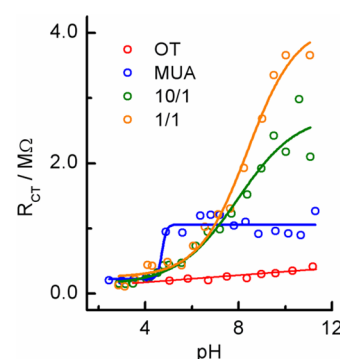


Figure 9. Charge transfer resistance (R_{CT}) of 1 mM $\text{Fe}(\text{CN})_6^{3-/4-}$ at the OT, MUA, and MUA/OT mixed layers at various solution pH values.

At pH below 5, the R_{CT} values are similar for all the layers studied. By taking into account the equivalence between the R_{CT} values and the electron transfer rate constant, a value of $k = 7 \pm 2 \times 10^{-6}$ cm/s is obtained in this pH region. This rate constant value is well within the limits of those typical for electron transfer of ferricyanide through an octane to decanethiol SAM considering only the tunneling mechanism,⁴² concluding that the layers act as blocking barriers for ferricyanide under these experimental conditions.

In the case of MUA-SAM, an important increase is observed that levels off around pH 5.5. This pH-dependent titration curve is ascribed to the electrostatic interactions between the terminal groups of the MUA monolayer (either protonated or deprotonated) and the negatively charged ferricyanide probe. It is then supposed that at pH > 5.5 the SAM head groups are deprotonated, resulting in an additionally higher charge transfer resistance for ferricyanide due to the electrostatic repulsion with the SAM surface. The inflection point of the titration curve for the MUA-SAM can be interpreted as the surface dissociation pK of the carboxylic acid groups in the SAM surface. This value of around 5.5 is very low in comparison with most of the data in literature that explain the change in the

surface pK of ω -carboxy-terminated SAMs with respect to the solution pK as being due to the stabilization of the protonated state by hydrogen bond formation in the adsorbed state.^{29,51–62} However, the extended literature in this topic concludes that the apparent pK values obtained are highly dependent on the measurement technique used for determination as well as experimental conditions such as solution ionic strength. One important factor to be taken into account is the SAM fabrication method, being most of the results reported on the spontaneously formed monolayers from ethanolic solutions. In the present case, there are two differences that are important to highlight. On one hand, the SAM is formed under electrochemical control and, therefore, is forced to reach a specific final estate. On the other, the layers are prepared from aqueous alkaline solutions from deprotonated carboxylate groups that should be accommodated in the surface of the as prepared layer. In this sense, it is not expected that the hydrogen bond can form in the same way as they do when the layers are built from protonated carboxylic groups that can interact through hydrogen bonds in the first moment of assembly contributing to stabilize the complete layer structure.

The behavior observed for the R_{CT} values measured with the mixed layers (molar ratios MUA:OT in the formation solution are 10:1 and 1:1) is somewhat intriguing. A displacement of the titration curves at higher pH together with an increase in the values of R_{CT} in alkaline solutions would indicate that the deprotonation of the carboxy terminal groups takes place at higher pH. This fact should be related to the different environment that the carboxylate group experiments in the proximity of the hydrophobic methyl terminal groups in the mixed layers. Moreover, the higher R_{CT} can be provoked not only by electrostatic repulsions but also by a major blocking to electron transfer due to a better organization of the molecules.

CONCLUSIONS

The surface composition of MUA:OT mixed layers formed from alkaline solutions under electrochemical control is directed by the magnitude of the oxidation potential of each component. In fact, the small difference of 115 mV between the anodic potential for adsorption of MUA and OT gives advantage to the chemisorption of OT, and therefore, the SAM composition is enriched in the component of lower adsorption potential. The adsorption behavior, as defined by the shape of the chemisorption peak, is also an important feature to be taken into account in the fabrication of the mixed layers. Bifunctional molecules present the problem of competitive adsorption through both terminal groups, and this is also evidenced in the final composition of the mixed SAM.

The mixed SAM properties can be improved by maintaining the layer in contact with blank electrolyte at controlled potential for a fixed time. As this step is carried out in the absence of free thiol molecules, the composition does not change but the molecules organize in the layer acting as an annealing of the SAM.

Under the experimental conditions of this work, we have been able to prepare mixed SAMs that show distinctive characteristics that can be defined as “macroscopically homogeneous” at high MUA:OT ratio and a “homogeneously mixed” at low MUA:OT ratio. The first one is considered to be formed by small domains that keep the same energetic as the single component SAM of the same thiol molecules, and the

second one is a monolayer containing a small amount of MUA molecules that are diluted within the OT organized layer.

The compactness of the mixed layers as stated by double-layer capacity measurements are in agreement with the evolution of reductive desorption potentials: the lower the SAM composition in MUA molecules, the more negative the reductive desorption potential and the lower the average relative permittivity.

Finally, the mixed SAMs modulate the charge transfer resistance of the ferricyanide redox probe in a pH-dependent fashion. The results are interpreted on the basis of changes in the protonation state of the carboxy terminal groups of the layers and higher blocking capacity.

AUTHOR INFORMATION

Corresponding Author

*E-mail: tpineda@uco.es; Ph +34-957-218646; Fax +34-957-218618 (T.P.).

Notes

The authors declare no competing financial interest.

ACKNOWLEDGMENTS

We thank the Ministerio de Economía y Competitividad (MINECO) (Project CTQ2010-16137), Junta de Andalucía (P10-FQM-6408), and University of Córdoba for financial support of this work.

REFERENCES

- (1) Dubois, L. H.; Nuzzo, R. G. Synthesis, Structure, and Properties of Model Organic Surfaces. *Annu. Rev. Phys. Chem.* **1992**, *43*, 437–463.
- (2) Nuzzo, R. G.; Zegarski, B. R.; Dubois, L. H. Fundamental Studies of the Chemisorption of Organosulfur Compounds on Au(111) - Implications for Molecular Self-Assembly on Gold Surfaces. *J. Am. Chem. Soc.* **1987**, *109*, 733–740.
- (3) Poirier, G. E. Characterization of Organosulfur Molecular Monolayers on Au(111) Using Scanning Tunneling Microscopy. *Chem. Rev.* **1997**, *97*, 1117–1127.
- (4) Ulman, A. Formation and Structure of Self-Assembled Monolayers. *Chem. Rev.* **1996**, *96*, 1533–1554.
- (5) Love, J. C.; Estroff, L. A.; Kriebel, J. K.; Nuzzo, R. G.; Whitesides, G. M. Self-Assembled Monolayers of Thiolates on Metals as a Form of Nanotechnology. *Chem. Rev.* **2005**, *105*, 1103–1169.
- (6) Vericat, C.; Vela, M. E.; Benitez, G.; Carro, P.; Salvarezza, R. C. Self-Assembled Monolayers of Thiols and Dithiols on Gold: New Challenges for a Well-Known System. *Chem. Soc. Rev.* **2010**, *39*, 1805–1834.
- (7) Dannenberger, O.; Weiss, K.; Himmel, H. J.; Jager, B.; Buck, M.; Woll, C. An Orientation Analysis of Differently Endgroup-Functionalised Alkanethiols Adsorbed on Au Substrates. *Thin Solid Films* **1997**, *307*, 183–191.
- (8) Kang, J. F.; Liao, S.; Jordan, R.; Ulman, A. Mixed Self-Assembled Monolayers of Rigid Biphenyl Thiols: Impact of Solvent and Dipole Moment. *J. Am. Chem. Soc.* **1998**, *120*, 9662–9667.
- (9) Kang, J. F.; Jordan, R.; Ulman, A. Wetting and Fourier Transform Infrared Spectroscopy Studies of Mixed Self-Assembled Monolayers of 4'-Methyl-4-Mercaptobiphenyl and 4'-Hydroxy-4-Mercaptobiphenyl. *Langmuir* **1998**, *14*, 3983–3985.
- (10) Hohman, J. N.; Zhang, P.; Morin, E. I.; Han, P.; Kim, M.; Kurland, A. R.; McClanahan, P. D.; Balema, V. P.; Weiss, P. S. Self-Assembly of Carboranethiol Isomers on Au{111}: Intermolecular Interactions Determined by Molecular Dipole Orientations. *ACS Nano* **2009**, *3*, 527–536.
- (11) Folkers, J. P.; Laibinis, P. E.; Whitesides, G. M.; Deutch, J. Phase-Behavior of 2-Component Self-Assembled Monolayers of Alkanethiolates on Gold. *J. Phys. Chem.* **1994**, *98*, 563–571.

- (12) Laibinis, P. E.; Nuzzo, R. G.; Whitesides, G. M. Structure of Monolayers Formed by Coadsorption of 2-Normal-Alkanethiols of Different Chain Lengths on Gold and its Relation to Wetting. *J. Phys. Chem.* **1992**, *96*, 5097–5105.
- (13) Kakiuchi, T.; Iida, M.; Gon, N.; Hobara, D.; Imabayashi, S.; Niki, K. Miscibility of Adsorbed 1-Undecanethiol and 11-Mercapto-undecanoic Acid Species in Binary Self-Assembled Monolayers on Au(111). *Langmuir* **2001**, *17*, 1599–1603.
- (14) Hobara, D.; Ota, M.; Imabayashi, S.; Niki, K.; Kakiuchi, T. Phase Separation of Binary Self-Assembled Thiol Monolayers Composed of 1-Hexadecanethiol and 3-Mercaptopropionic Acid on Au(111) Studied by Scanning Tunneling Microscopy and Cyclic Voltammetry. *J. Electroanal. Chem.* **1998**, *444*, 113–119.
- (15) Imabayashi, S.; Gon, N.; Sasaki, T.; Hobara, D.; Kakiuchi, T. Effect of Nanometer-Scale Phase Separation on Wetting of Binary Self-Assembled Thiol Monolayers on Au(111). *Langmuir* **1998**, *14*, 2348–2351.
- (16) Brett, C. M. A.; Kresak, S.; Hianik, T.; Brett, A. M. O. Studies on Self-Assembled Alkanethiol Monolayers Formed at Applied Potential on Polycrystalline Gold Electrodes. *Electroanalysis* **2003**, *15*, 557–565.
- (17) Diao, P.; Hou, Q. C.; Guo, M.; Xiang, M.; Zhang, Q. Effect of Substrate Potentials on the Structural Disorders of Alkanethiol Monolayers Prepared by Electrochemically Directed Assembly. *J. Electroanal. Chem.* **2006**, *597*, 103–110.
- (18) Ma, F. Y.; Lennox, R. B. Potential-Assisted Deposition of Alkanethiols on Au: Controlled Preparation of Single- and Mixed-Component SAMs. *Langmuir* **2000**, *16*, 6188–6190.
- (19) Paik, W. K.; Eu, S.; Lee, K.; Chon, S.; Kim, M. Electrochemical Reactions in Adsorption of Organosulfur Molecules on Gold and Silver: Potential Dependent Adsorption. *Langmuir* **2000**, *16*, 10198–10205.
- (20) Weisshaar, D. E.; Lamp, B. D.; Porter, M. D. Thermodynamically Controlled Electrochemical Formation of Thiolate Monolayers at Gold: Characterization and Comparison to Self-Assembled Analogs. *J. Am. Chem. Soc.* **1992**, *114*, 5860–5862.
- (21) Sumi, T.; Uosaki, K. Electrochemical Oxidative Formation and Reductive Desorption of a Self-Assembled Monolayer of Decanethiol on a Au(111) Surface in KOH Ethanol Solution. *J. Phys. Chem. B* **2004**, *108*, 6422–6428.
- (22) Sumi, T.; Wano, H.; Uosaki, K. Electrochemical Oxidative Adsorption and Reductive Desorption of a Self-Assembled Monolayer of Decanethiol on the Au(111) Surface in KOH plus Ethanol Solution. *J. Electroanal. Chem.* **2003**, *550*, 321–325.
- (23) Meunier-Prest, R.; Legay, G.; Raveau, S.; Chiffot, N.; Finot, E. Potential-Assisted Deposition of Mixed Alkanethiol Self-Assembled Monolayers. *Electrochim. Acta* **2010**, *55*, 2712–2720.
- (24) Qu, D.; Morin, M. The Kinetics of the Electroformation of a Self-Assembled Monolayer of Butanethiols on Gold. *J. Electroanal. Chem.* **2002**, *524*, 77–80.
- (25) Rifai, S.; Lopinski, G. P.; Ward, T.; Wayner, D. D. M.; Morin, M. Electrochemically Driven Assembly of Mixed Dithiol Bilayers via Sulfur Dimers. *Langmuir* **2003**, *19*, 8916–8921.
- (26) Rifai, S.; Morin, M. Isomeric Effect on the Oxidative Formation of Bilayers of Benzenedimethanethiol on Au(111). *J. Electroanal. Chem.* **2003**, *550*, 277–289.
- (27) Garcia-Raya, D.; Madueno, R.; Blazquez, M.; Pineda, T. Formation of 1,8-Octanedithiol Mono- and Bilayers under Electrochemical Control. *J. Phys. Chem. C* **2010**, *114*, 3568–3574.
- (28) Walczak, M. M.; Chung, C. K.; Stole, S. M.; Widrig, C. A.; Porter, M. D. Structure and Interfacial Properties of Spontaneously Adsorbed Normal-Alkanethiolate Monolayers on Evaporated Silver Surfaces. *J. Am. Chem. Soc.* **1991**, *113*, 2370–2378.
- (29) Ramirez, P.; Andreu, R.; Cuesta, A.; Calzado, C. J.; Calvente, J. J. Determination of the Potential of Zero Charge of Au(111) Modified with Thiol Monolayers. *Anal. Chem.* **2007**, *79*, 6473–6479.
- (30) Zelenay, P.; Waszczuk, P.; Dobrowolska, K.; Sobkowski, J. Adsorption of Benzoic-Acid on a Polycrystalline Gold Electrode. *Electrochim. Acta* **1994**, *39*, 655–660.
- (31) Li, H. Q.; Roscoe, S. G.; Lipkowski, J. FTIR Studies of Benzoate Adsorption on the Au(111) Electrode. *J. Electroanal. Chem.* **1999**, *478*, 67–75.
- (32) Corrigan, D. S.; Krauskopf, E. K.; Rice, L. M.; Wieckowski, A.; Weaver, M. J. Adsorption of Acetic-Acid at Platinum and Gold Electrodes - A Combined Infrared and Radiotracer Study. *J. Phys. Chem.* **1988**, *92*, 1596–1601.
- (33) Paik, W. K.; Han, S. B.; Shin, W.; Kim, Y. S. Adsorption of Carboxylic Acids on Gold by Anodic Reaction. *Langmuir* **2003**, *19*, 4211–4216.
- (34) Kakiuchi, T.; Usui, H.; Hobara, D.; Yamamoto, M. Voltammetric Properties of the Reductive Desorption of Alkanethiol Self-Assembled Monolayers from a Metal Surface. *Langmuir* **2002**, *18*, 5231–5238.
- (35) Hatchett, D. W.; Uibel, R. H.; Stevenson, K. J.; Harris, J. M.; White, H. S. Electrochemical Measurement of the Free Energy of Adsorption of n-Alkanethiolates at Ag(111). *J. Am. Chem. Soc.* **1998**, *120*, 1062–1069.
- (36) Azeahara, H.; Yoshimoto, S.; Hokari, H.; Akiba, U.; Taniguchi, I.; Fujihira, M. Investigation of the Structure of Self-Assembled Monolayers of Asymmetrical Disulfides on Au(111) Electrodes by Electrochemical Desorption. *J. Electroanal. Chem.* **1999**, *473*, 68–74.
- (37) Widrig, C. A.; Chung, C.; Porter, M. D. The Electrochemical Desorption of n-Alkanethiol Monolayers from Polycrystalline Au and Ag Electrodes. *J. Electroanal. Chem.* **1991**, *310*, 335–359.
- (38) Smith, C. P.; White, H. S. Voltammetry of Molecular Films Containing Acid-Base Groups. *Langmuir* **1993**, *9*, 1–3.
- (39) Sanders, W.; Vargas, R.; Anderson, M. R. Characterization of Carboxylic Acid-Terminated Self-Assembled Monolayers by Electrochemical Impedance Spectroscopy and Scanning Electrochemical Microscopy. *Langmuir* **2008**, *24*, 6133–6139.
- (40) Jin, B.; Wang, G.-X.; Millo, D.; Hildebrandt, P.; Xia, X.-H. Electric-Field Control of the pH-Dependent Redox Process of Cytochrome c Immobilized on a Gold Electrode. *J. Phys. Chem. C* **2012**, *116*, 13038–13044.
- (41) Porter, M. D.; Bright, T. B.; Allara, D. L.; Chidsey, C. E. D. Spontaneously Organized Molecular Assemblies. 4. Structural Characterization of n-Alkyl Thiol Monolayers on Gold by Optical Ellipsometry, Infrared Spectroscopy, and Electrochemistry. *J. Am. Chem. Soc.* **1987**, *109*, 3559–3568.
- (42) Miller, C.; Cuendet, P.; Gratzel, M. Adsorbed Omega-Hydroxy Thiol Monolayers on Gold Electrodes - Evidence for Electron-Tunneling to Redox Species in Solution. *J. Phys. Chem.* **1991**, *95*, 877–886.
- (43) Bain, C. D.; Troughton, E. B.; Tao, Y. T.; Evall, J.; Whitesides, G. M.; Nuzzo, R. G. Formation of Monolayer Films by the Spontaneous Assembly of Organic Thiols from Solution onto Gold. *J. Am. Chem. Soc.* **1989**, *111*, 321–335.
- (44) Cannes, C.; Kanoufi, F.; Bard, A. J. Cyclic Voltammetry and Scanning Electrochemical Microscopy of Ferrocenemethanol at Monolayer and Bilayer-Modified Gold Electrodes. *J. Electroanal. Chem.* **2003**, *547*, 83–91.
- (45) Chidsey, C. E. D.; Loiacono, D. N. Chemical Functionality in Self-Assembled Monolayers: Structural and Electrochemical Properties. *Langmuir* **1990**, *6*, 682–691.
- (46) Molinero, V.; Calvo, E. J. Electrostatic Interactions at Self-Assembled Molecular Films of Charged Thiols on Gold. *J. Electroanal. Chem.* **1998**, *445*, 17–25.
- (47) Takehara, K.; Takemura, H.; Ide, Y. Electrochemical Studies of the Terminally Substituted Alkanethiol Monolayers Formed on a Gold Electrode - Effects of the Terminal Group on the Redox Responses of $\text{Fe}(\text{CN})_6^{3-}$, $\text{Ru}(\text{NH}_3)_6^{3+}$ and Ferrocenedimethanol. *Electrochim. Acta* **1994**, *39*, 817–822.
- (48) Degefa, T. H.; Schon, P.; Bongard, D.; Walder, L. Elucidation of the Electron Transfer Mechanism of Marker Ions at SAMs with Charged Head Groups. *J. Electroanal. Chem.* **2004**, *574*, 49–62.
- (49) Campina, J. M.; Martins, A.; Silva, F. Selective Permeation of a Liquidlike Self-Assembled Monolayer of 11-Amino-1-undecanethiol

on Polycrystalline Gold by Highly Charged Electroactive Probes. *J. Phys. Chem. C* **2007**, *111*, 5351–5362.

(50) Bard, A. J.; Faulkner, L. R. *Electrochemical Methods: Principles and Applications*, 2nd ed.; John Wiley and Sons: New York, 2001.

(51) Burgess, I.; Seivewright, B.; Lennox, R. B. Electric Field Driven Protonation/Deprotonation of Self-Assembled Monolayers of Acid-Terminated Thiols. *Langmuir* **2006**, *22*, 4420–4428.

(52) White, H. S.; Peterson, J. D.; Cui, Q. Z.; Stevenson, K. J. Voltammetric Measurement of Interfacial Acid/Base Reactions. *J. Phys. Chem. B* **1998**, *102*, 2930–2934.

(53) Creager, S. E.; Clarke, J. Contact-Angle Titrations of Mixed Omega-Mercaptoalkanoic Acid Alkanethiol Monolayers on Gold - Reactive vs Nonreactive Spreading, and Chain-Length Effects on Surface pKa Values. *Langmuir* **1994**, *10*, 3675–3683.

(54) Andreu, R.; Fawcett, W. R. Discreteness-of-Charge Effects at Molecular Films Containing Acid/Base Groups. *J. Phys. Chem.* **1994**, *98*, 12753–12758.

(55) Zhao, J. W.; Luo, L. Q.; Yang, X. R.; Wang, E. K.; Dong, S. J. Determination of Surface pKa of SAM Using an Electrochemical Titration Method. *Electroanalysis* **1999**, *11*, 1108–1111.

(56) Smith, D. A.; Wallwork, M. L.; Zhang, J.; Kirkham, J.; Robinson, C.; Marsh, A.; Wong, M. The Effect of Electrolyte Concentration on the Chemical Force Titration Behavior of Omega-Functionalized SAMs: Evidence for the Formation of Strong Ionic Hydrogen Bonds. *J. Phys. Chem. B* **2000**, *104*, 8862–8870.

(57) Kakiuchi, T.; Iida, M.; Imabayashi, S.; Niki, K. Double-Layer-Capacitance Titration of Self-Assembled Monolayers of Omega-Functionalized Alkanethiols on Au(111) Surface. *Langmuir* **2000**, *16*, 5397–5401.

(58) Sugihara, K.; Shimazu, K.; Uosaki, K. Electrode Potential Effect on the Surface pKa of a Self-Assembled 15-Mercaptohexadecanoic Acid Monolayer on a Gold/Quartz Crystal Microbalance Electrode. *Langmuir* **2000**, *16*, 7101–7105.

(59) Smalley, J. F.; Chalfant, K.; Feldberg, S. W.; Nahir, T. M.; Bowden, E. F. An Indirect Laser-Induced Temperature Jump Determination of the Surface pKa of 11-Mercaptoundecanoic Acid Monolayers Self-Assembled on Gold. *J. Phys. Chem. B* **1999**, *103*, 1676–1685.

(60) Smalley, J. F. Indirect Laser-Induced Temperature Jump Study of the Chain-Length Dependence of the pK(a)'s of Omega-Mercaptoalkanoic Acid Monolayers Self-Assembled on Gold. *Langmuir* **2003**, *19*, 9284–9289.

(61) Ramirez, P.; Granero, A.; Andreu, R.; Cuesta, A.; Mulder, W. H.; Jose Calvente, J. Potential of Zero Charge as a Sensitive Probe for the Titration of Ionizable Self-Assembled Monolayers. *Electrochem. Commun.* **2008**, *10*, 1548–1550.

(62) Luque, A. M.; Mulder, W. H.; Jose Calvente, J.; Cuesta, A.; Andreu, R. Proton Transfer Voltammetry at Electrodes Modified with Acid Thiol Monolayers. *Anal. Chem.* **2012**, *84*, 5778–5786.